Dense Gas Phenomena in a Free-Piston Hypersonic Wind Tunnel

K. R. ENKENHUS* AND C. PARAZZOLI†
von Kármán Institute for Fluid Dynamics, Rhode-Saint-Genèse, Belgium

A theoretical and experimental study has been made of dense gas effects in the VKI Longshot M = 15–27 high Reynolds number tunnel. Longshot differs from a conventional gun tunnel in that the nitrogen test gas compressed by a heavy piston is trapped in a reservoir at the end of the barrel at peak pressure and temperature (typically 30,000 psi at 2150°K) by the closing of a system of check valves as the piston rebounds. The supply conditions decay gradually during the 25 msec running time as the gas flows through the nozzle from the finite reservoir volume. Theoretical analyses, which account for real gas effects due to intermolecular forces and vibrational excitation, are presented for the free-piston cycle, the decay of reservoir conditions, and the flow through the hypersonic nozzle. Experimental data are found to agree well with predictions.

Nomenclature

a = sound speed
A = cross-sectional area
D = diameter
e = internal energy per unit mass
h = enthalpy per unit mass
m = mass
M = Mach number
p = pressure
R = gas constant per unit mass
s = entropy per unit mass
t = time
T = temperature
v = velocity
V = volume
x = distance
α,β = constants in Van der Waals equation
γ = ratio of specific heats
ρ = density

Superscripts

(˙) = time derivative

Subscripts

0 = reservoir
1 = barrel
2 = behind primary shock
3 = behind piston
4 = driver
5 = behind reflected shock
i,f = initial and final, respectively
p = piston
s = shock
v = valve
yz = $\partial y/\partial z$ (partial derivatives)
$*$ = sonic

I. Introduction

THE VKI Longshot free-piston hypersonic tunnel[1] was designed and originally operated by Perry and his associates at Republic Aviation[2,3] with the goal of attaining the high supply pressures needed for the experimental study of turbulent heating and flow separation under re-entry conditions. A planned facility modification to raise the maximum supply pressure from the current value of 50,000 psi to 200,000 psi will permit free-flight Mach and Reynolds numbers to be achieved for the critical portion of the re-entry trajectory of a 6000 mile range ICBM with a ballistic coefficient of 1000 lb/ft², for a 7-ft-long vehicle. The feasibility of operating at 200,000 psi has been confirmed by tests of a pilot facility,[4] but very little design data for such conditions exists.

The operating principle of Longshot may be understood from Fig. 1, which shows the basic features and dimensions of the facility, and the compression cycle. The key to the high performance lies, first, in the use of a relatively heavy (5 lb) piston to compress the nitrogen test gas to high peak values of pressure and temperature; and, second, in trapping this gas in a reservoir at the end of the barrel at essentially peak conditions by the closing of a system of check valves as the piston begins to rebound.

As the pressure in the reservoir rises, a plastic plug is blown out of the nozzle throat and hypersonic flow is initiated in the pre-evacuated open-jet test section. Mach numbers from 15 to 27 may be obtained by using throat inserts of different sizes. The supply conditions decay moderately during the 25 msec running time as the stored gas exhausts through the nozzle throat.

In facilities which operate at very high pressures, aerodynamic performance is significantly influenced by departures from the perfect gas law due to dense-gas effects. For the achievable range of operating temperatures in Longshot, there are no chemical reactions in the nitrogen test gas, but the effect of energy storage in molecular vibration must also be taken into account.

The purpose of this paper is to present the results of theoretical and experimental investigations of these phenomena in the Longshot tunnel, which may be applied to design and performance studies of related facilities. The problems that are treated in turn are 1) the free-piston cycle, 2) the decay of supply conditions as the gas trapped in the reservoir exhausts through the nozzle, and 3) the flow processes in the nozzle.

II. Piston Cycle

A. Dense Gas Model and Method of Analysis

Although an elaborate calculation of the Longshot piston cycle by numerical integration of the characteristics equations for one-dimensional flow has been carried out in the past,[4] good agreement with experimental measurements was not obtained because of the assumption of a thermally and

Presented as Paper 69-169 at the AIAA 7th Aerospace Sciences Meeting, New York, January 20–22, 1969; submitted January 23, 1969; revision received June 12, 1969.

* Professor of Physics. Member AIAA.
† Diploma student. Student Member AIAA.

calorically perfect gas. The present method of analysis reduces the problem to the solution of a system of ordinary differential equations by making a number of simplifying assumptions which are valid for Longshot, and includes appropriate real gas effects.

Real gas effects in nitrogen were approximately accounted for by assuming a vibrationally excited Van der Waals gas in thermodynamic equilibrium. The equation of state is

$$p(\rho,T) = RT/(\rho^{-1} - \beta) - \alpha\rho^2 \tag{1}$$

The isentrope is

$$\tfrac{7}{2}\ln T + \Gamma(T) - \ln(p + \alpha\rho^2) = \text{const} \tag{2}$$

where

$$\Gamma(T) = (\theta_v/T)/(1 - e^{-\theta_v/T}) - \ln(e^{\theta_v/T} - 1) \tag{3}$$

is the contribution to the entropy due to vibrational excitation. θ_v is the characteristic vibrational temperature.

The sound speed is derivable from Eqs. (1–3) as

$$\left.\begin{aligned} a(p,\rho,T) = (p_\rho)_s^{0.5} &= \left[\frac{2\alpha\rho(p + \alpha\rho^2)^{-1} - GT_\rho}{GT_p - (p + \alpha\rho^2)^{-1}}\right]^{0.5} \\ \text{where} \\ G &= 3.5/T + T^{-1}(\theta_v/T)^2(e^{\theta_v/T} - 1)^{-2}e^{\theta_v/T} \end{aligned}\right\} \tag{4}$$

The partial derivatives T_ρ and T_p are readily obtainable from the equation of state.

The internal energy per unit mass is

$$e(\rho,T) = 2.5RT + R\theta_v(e^{\theta_v/T} - 1)^{-1} - \alpha\rho \tag{5}$$

and the enthalpy is $h(p,\rho,T) = e + p/\rho$.

The method of calculating the piston cycle[5] will be now outlined. A basic assumption is that the significant part of the entropy rise of the test gas occurs when it is traversed by the primary and first reflected shocks. Additional entropy increases due to further shock reflections, and frictional losses in the check valve system, are neglected. The principal steps in the calculation are, therefore:

1) Integration of the equation of motion to determine the speed of the piston when it is struck by the first reflected shock. In this calculation, chambrage is ignored to permit the pressure on the base of the piston to be related to the pressure in the driver gas by the expression for a simple rarefaction wave in a dense gas. This procedure is valid in the absence of chambrage because the reflected rarefaction wave does not overtake the piston during its stroke. The speed of the piston is then corrected for chambrage effects using results based on the analysis of high-speed guns, including dense gas effects.

2) Calculation of the pressure and temperature in the gas behind the reflected shock. Perfect gas theory is used to find the strength of the primary and reflected shocks and the pressure p_{5i} and temperature T_{5i} behind the reflected shock at the time it strikes the piston face, since the pressures and temperatures involved are moderate.

3) Determination of the final reservoir conditions (p_{0f}, T_{0f}) resulting from an isentropic real-gas compression in which the kinetic energy of the piston is transferred to the gas as the piston is brought to rest. Calculation of the flow in the check valve system for current operating conditions shows that p_{0f} and T_{0f} are nearly equal to the values which would result neglecting the flow constriction produced by the valves. When the valve flow losses are ignored, the final reservoir conditions are obtainable for a given piston speed by solving a set of algebraic equations.

B. Prediction of Piston Speed

The piston speed and position is first obtained neglecting chambrage by solving the differential equations

$$\dot{v}_p = (p_3 - p_2)A_1/m_p \text{ (Newton's law)} \tag{6}$$

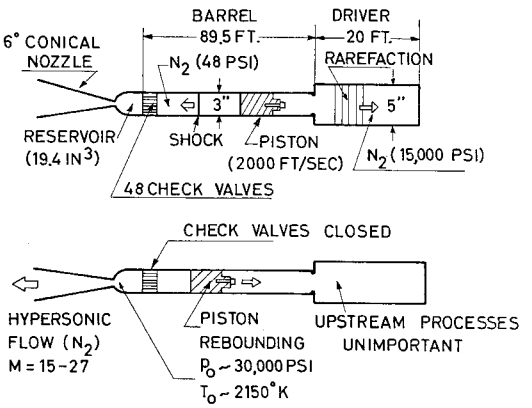

Fig. 1 Longshot compression cycle.

$$\dot{x} = v_p \tag{7}$$

$$\dot{p}_3 = -a_3\rho_3\dot{v}_p \text{ (simple wave)} \tag{8}$$

$$\dot{\rho}_3 = a_3^{-2}\dot{p}_3 \text{ (isentropic flow)} \tag{9}$$

$$\dot{T}_3 = p_{T_3}^{-1}(1 - a_3^{-2}p_{\rho_3})\dot{p}_3 \text{ (state)} \tag{10}$$

It is assumed that the pressure acting on the front of the piston is equal to that behind the primary shock, and that the particle velocity behind the shock equals v_p. Perfect gas shock wave theory[6] then gives

$$p_2(v_p) = p_1\{1 + 4\gamma_1\sigma(\sigma + [1 + \sigma^2]^{0.5})/(\gamma_1 + 1)\} \tag{11}$$

where $\sigma = (\gamma_1 + 1)v_p/4a_1$.

The integration of Eqs. (6–10) is started at $t = 0$ with the initial conditions $x = v_p = 0$ and $(p_3,\rho_3,T_3) = (p_4,\rho_4,T_4)$, and terminated at $x = x_i$ when the piston is struck by the first reflected shock. From mass continuity considerations, x_i is expressible in terms of the barrel length x_1 and conditions in region 5 behind the reflected shock by

$$x_i = x_1[1 - (p_1/p_{5i})(T_{5i}/T_1)] \tag{12}$$

The pressure and temperature ratios appearing in this equation are calculated using the well-known perfect gas reflected shock equations[6] for the corresponding value of the primary shock Mach number

$$M_s(v_{pi}) = \sigma + (1 + \sigma^2)^{0.5} \tag{13}$$

Integration of the equations must, in general, be carried out numerically. However, if the driver gas is only moderately dense ($\alpha\rho^2/p$ and $\beta\rho \ll 1$ in Van der Waals equation) and the driver gas is cold (no vibrational excitation) an approximate analytical solution for the piston motion for a Van der Waals gas can be obtained[5] by a method first applied to a perfect gas by Stalker.[7]

The value of v_{pi} is now corrected for chambrage, and after doing so, the conditions in region 5 are recalculated using the corrected piston speed. A correlation of perfect gas high-speed gun calculations[8] indicates that the piston speed is increased by chambrage in the ratio $1 + [1 - (D_1/D_4)^2]\gamma_4/6$. This value may be multiplied by an additional factor ϵ to allow for dense gas effects, which further increase the performance of a chambered gun. On the basis of an analysis of dense gas effects on the limiting piston speed obtainable in a gun with infinite chambrage,[5]

$$\epsilon = \frac{(1 + C\rho'_4)(1 + 2\rho'_4/\gamma_4)^{0.5}}{\{1 + 2C\rho'_4(\gamma_4 + 1)/\gamma_4 + [C/(\gamma_4 - 1)]^{1/\gamma_4}\rho'_4\}^{0.5}} \tag{14}$$

where

$$C = [2/(\gamma_4 + 1)]^{\gamma_4/(\gamma_4 - 1)}$$

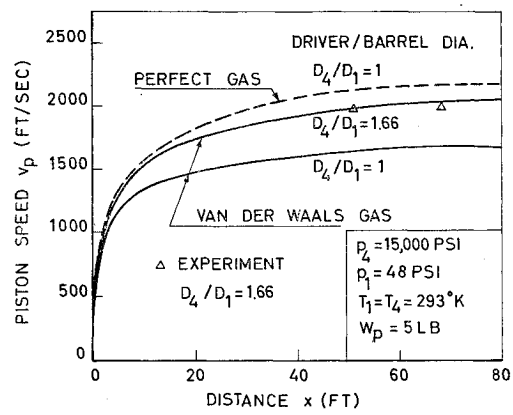

Fig. 2 Comparison of predicted and measured piston speed.

and

$$\rho'_4 = (\gamma_4 - 1)\beta p_4/2RT_4$$

This result is based on an Abel-Noble gas and may be expected to overestimate the correction, since attractive intermolecular forces are neglected.

Experimental measurements[9] of the piston speed and pressure variation with time in the barrel were made using five Kistler piezo-electric pressure transducers mounted at appropriate positions. The signals were amplified and recorded on oscilloscopes. Figure 2 shows a comparison of the predicted and measured piston speed for representative initial conditions. It may be seen that when chambrage effects are neglected ($D_4/D_1 = 1$), perfect gas theory slightly overestimates the piston speed, whereas the Van der Waals theory greatly underestimates it. It is well known that dense gas effects reduce the projectile velocity in an unchambered gun due to the predominance of intermolecular attractive forces.[8] The calculation made for a Van der Waals gas including chamberage effects is in good agreement with measurements.

C. Final Compression Process

The final compression process is shown schematically in Fig. 3. The differential equations governing the gas ahead of the piston are as follows:

$$\dot{v}_p = (p_{3i} - p_5)A_1/m_p \text{ (Newton's law)} \quad (15)$$

$$\dot{\rho}_5 = (\rho_5 v_p - \dot{m}/A_1)/x_5 \text{ (continuity)} \quad (16)$$

together with the relation $\dot{x}_5 = -v_p$ and the isentropic flow and state relations, Eqs. (9) and (10), respectively, written for region 5.

The corresponding equations for the gas in the reservoir are

$$\dot{\rho}_0 = \dot{m}/V_0 \quad (17)$$

$$\dot{T}_0 = e_{T_0}{}^{-1}[\rho_0{}^{-1}(e_5 - e_0 - \rho_0 e_{\rho_0})\dot{\rho}_0 + p_5 A_1 v_p/\rho_0 V_0 - (\rho_5 A_1 x_5)(e_{\rho_5}\dot{\rho}_5 + e_{T_5}\dot{T}_5)/\rho_0 V_0] \quad (18)$$

and the state relation, Eq. (1), which yields $p_0 = p_0(\rho_0, T_0)$. Equation (18) is derivable by applying the conservation of energy to a control volume containing all the test gas.

The mass flux through the valves is

$$\dot{m} = \rho_v v_v A_v \quad (19)$$

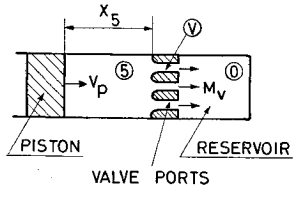

Fig. 3 Valve flow analysis.

where

$$v_v = [2(h_5 - h_v)]^{0.5} \quad (20)$$

and

$$\rho_v = \int_{p_5}^{p_v} a^{-2}dp + \rho_5 \quad (21)$$

The determination of the sound speed in Eq. (21) requires that the temperature be known; it is given by

$$T = T_5 + \int_{p_5}^{p} p_T{}^{-1}(1 + a^{-2}p_\rho)dp \quad (22)$$

Equations (21) and (22) are integrated simultaneously until the flow becomes choked ($M_v = v_v/a_v = 1$) or until $p_v = p_0$.

A valve flow calculation made (for simplicity) with a perfect gas using the equations presented in this section is shown in Fig. 4. Time $t = 0$ corresponds to the initial values of the variables when the piston is struck by the first reflected shock. It is assumed that the initial pressure and temperature in the reservoir are the same as in front of the piston. The calculation terminates after piston rebound, when $p_{0f} = p_5$ at valve closure. A study of the results shows that from the present test conditions and facility geometry, 1) p_0 and T_0 differ only slightly from p_5 and T_5 during the compression, and 2) the final reservoir conditions p_{0f} and T_{0f} are very nearly equal to the values of p_5 and T_5 which would be calculated when the piston comes to rest with no valve constrictions.

In the limiting case where the flow through the valves need not be considered, the final conditions for a vibrationally excited Van der Waals gas may be obtained by solving a set of algebraic equations, as described below.

The conservation of energy requires that the increase in internal energy of the test gas should equal the kinetic energy lost by the piston as it is brought to rest, plus the work done by the pressure force on the back of the piston

$$\rho_1 A_1 x_1 \Delta e = \tfrac{1}{2}m_p v_{p_i}{}^2 + p_3 A_1(x_f - x_i) \quad (23)$$

Since the last term in this equation is small, the further approximation is made that $p_3 = p_{3i}$ during the final compression stroke.

The position x_f at which the piston comes to rest is obtainable by substituting the continuity relation

$$\rho_{0f} = \rho_1 x_1(x_1 - x_f) \quad (24)$$

into the isentrope, Eq. (2). This yields

$$x_f = x_1(1 - \rho_1\beta) - (T_{5i}/T_{0f})^{2.5}x \times [x_1(1 - \rho_1\beta) - x_i] \exp\{\Gamma(T_{5i}) - \Gamma(T_{0f})\} \quad (25)$$

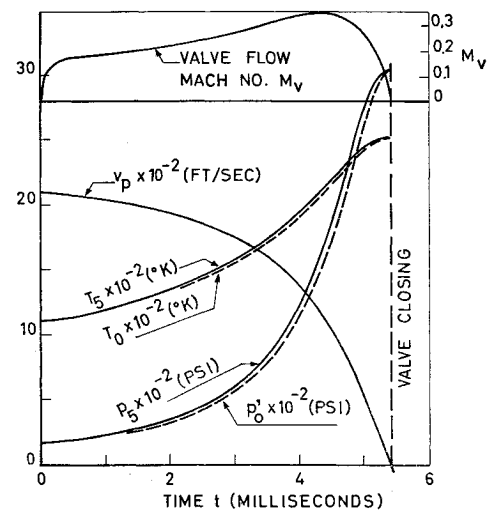

Fig. 4 Calculated longshot valve flow (perfect gas).

The change in internal energy is, by Eq. (5),

$$\Delta e = 2.5R(T_{0f} - T_{5i}) + R\theta_v[(e^{\theta_v/T_{0f}} - 1)^{-1} - (e^{\theta_v/T_{5i}} - 1)^{-1}] - \alpha(\rho_{0f} - \rho_{5i}) \quad (26)$$

Substitution of Eqs. (24–26) into Eq. (23) now leads to an implicit equation in the single unknown T_{0f}. x_f, ρ_{0f}, and p_{0f} may then be calculated in turn from Eqs. (25, 24, and 1).

Experimental measurements of the final reservoir pressure and temperature are compared with the aforementioned prediction method in Figs. 5 and 6. The pressure was measured with a Kistler gage, and the temperature with a tungsten-rhenium thermocouple. In these tests, the nozzle throat was blocked, and the temperature in the reservoir, after reaching the maximum value at valve closure, decayed slowly enough (~8°K/msec) so that the response of the thermocouple was adequate for an accurate determination of T_{0f}. The experimental points represent data obtained at driver pressures of 10,000 and 15,000 psi. The agreement with the theory including dense gas effects is seen to be good.

III. Decay of Supply Conditions

The variation of reservoir density ρ_0 with time t as the stored gas flows through the nozzle throat is given by the mass flow continuity equation,

$$\frac{t}{\tau} = -\int_{\rho_{0i}}^{\rho_0} g(\rho_0)\frac{d\rho_0}{\rho_0} \quad (27)$$

where $g(\rho_0) = [(\rho_*/\rho_0)(a_*/a_0)a_0/a_{0i}]^{-1}$, and $\tau = V_0/a_{0i}A_*$ is a characteristic decay time.

The process is assumed to be governed by steady flow equations because the time required for a disturbance to traverse the reservoir is small compared to τ. To a first approximation, the process may also be assumed isentropic since the temperature fall due to radiation losses to the reservoir walls is small during the run.

The problem is analyzed using a simple dense gas model (an Abel-Noble gas with no vibrational excitation) because this permits an approximate analytical solution to be obtained. The gas properties are given by Eqs. (1–5) with $\alpha = \theta_v = 0$. The isentrope, Eq. (2), can then be written with the aid of Eq. (1) as

$$p_0/p_{0i} = [(\rho_0/\rho_{0i})(1 - \beta\rho_{0i})/(1 - \beta\rho_0)]^\gamma \quad (28)$$

Values of the covolume β and effective ratio of specific heats γ were obtained by matching the equation of state and isentrope to a Mollier chart for dense nitrogen for the appropriate range of conditions.

The equations cited, together with the energy relation $h + v^2/2 = h_0$ and the condition $v_* = a_*$ at the nozzle throat yield expressions for the quantities appearing in the integrand $g(\rho_0)$ in Eq. (27). An approximate analytical solution is then obtainable assuming a moderate gas density ($\beta\rho \ll 1$). In terms involving $\beta\rho_*$, ρ_* is assumed to be expressible in terms of ρ_0 using the perfect gas relationship. When a binomial expansion of $g(\rho_0)$ is performed, retaining only the first-order term in $\beta\rho_0$, Eq. (27) may be integrated, with the result

$$\frac{\rho_0}{\rho_{0i}} = \left[\frac{1 + C_1 + C_2(1 - \beta\rho_{0i})^{(\gamma-1)/2}t/\tau}{1 + C_1(1 + C_2 t/\tau)^{-2/(\gamma-1)}}\right]^{-2/(\gamma-1)}$$

where

$$C_1 = \left(\frac{\gamma-1}{3-\gamma}\right)\left(\frac{\gamma+1}{2\gamma}\right)\times\left[\gamma + 1 - 2\left(\frac{2}{\gamma+1}\right)^{1/(\gamma-1)}\right]\beta\rho_{0i}$$

$$C_2 = \frac{\gamma-1}{2}\left(\frac{2}{\gamma+1}\right)^{(\gamma+1)/2(\gamma-1)}$$

$$\tau = V/A_*(\gamma RT_{0i})^{0.5} \quad (29)$$

τ is defined here to have the same value as in the perfect gas case. The corresponding pressure decay is obtained from Eq. (28) and the temperature decay is found using the equation of state. Calculations have shown that this approximate analytical solution agrees well with an exact numerical solution to the problem, even under conditions when $\beta\rho_0$ is not small compared with unity.[10]

The measured reservoir pressure vs time is compared with theory in Fig. 7. A large nozzle throat was used in order to obtain an easily measurable decay. The figure shows that the decay of supply pressure is much more rapid than predicted for a perfect gas, and somewhat more rapid than calculated for the isentropic expansion of an Abel-Noble gas. However, when the predicted pressure decay rate is increased by 0.42%/msec to allow for temperature losses due to radiation in the reservoir (a value experimentally determined in a separate run with the nozzle throat blocked),[10] good agreement between the theoretical and measured values results.

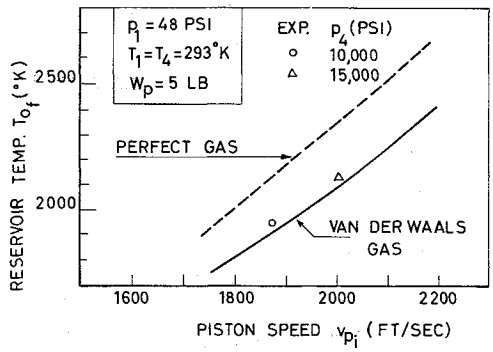

Fig. 6 Reservoir temperature.

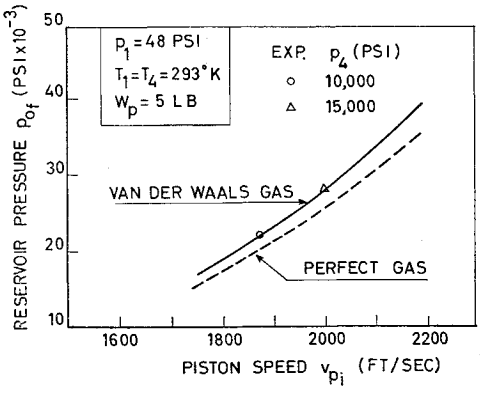

Fig. 5 Reservoir pressure.

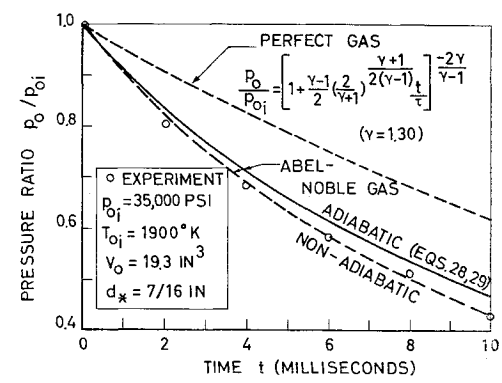

Fig. 7 Decay of supply pressure with time.

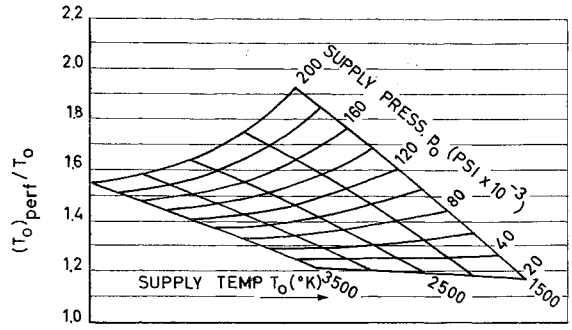

Fig. 8 Equivalent perfect gas supply temperature.

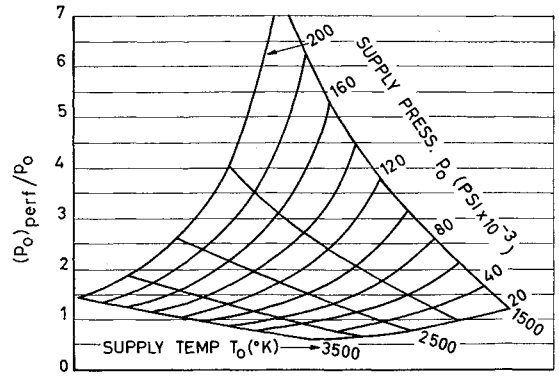

Fig. 9 Equivalent perfect gas supply pressure.

IV. Dense Gas Nozzle Flow

At the elevated supply pressures and temperatures at which Longshot operates, the expansion process in the nozzle is strongly influenced by real gas effects. The expansion process may be calculated assuming that the gas remains in thermodynamic equilibrium, since the work of previous investigators[11] shows that for Longshot conditions, vibrational freezing will not occur until the static temperature has fallen to a few hundred degrees Kelvin, where the energy remaining in the vibrational mode is small.

In order to calculate the expansion process and determine test section conditions for data reduction, accurate formulas for the equilibrium thermodynamic properties of nitrogen are required. Analytical expressions for the compressibility, internal energy, enthalpy, entropy, specific heats, and sound speed of real nitrogen have been derived by Culotta and Enkenhus.[12] These are obtained using general thermodynamic relations from two carefully-selected equations of state which apply below and above the critical density, respectively. The formulas give results which agree with the tables of Grabau and Brahinsky[13] with an average error of less than 1% (0.2% in s/R) from 300°K to 5000°K and densities from 1 to 1000 amagats.

The problem of determining the test section conditions corresponding to given supply conditions is simplified at hypersonic test section Mach numbers by the fact that the flow expands until it behaves like a perfect gas. Calculations of test section static conditions may therefore be made using an equivalent perfect gas supply pressure, $(p_0)_{perf}$, and supply temperature, $(T_0)_{perf}$, which correspond to the same entropy s_0/R and stagnation enthalpy h_0 as the real flow. The equivalent perfect gas supply conditions are given for nitrogen by

$$(T_0)_{perf} = h_0/3.5R \tag{30}$$

$$(p_0)_{perf} = \exp[3.5 \ln(T_0)_{perf} + 3.13793 - s_0/R] \tag{31}$$

In Eq. (31), $(T_0)_{perf}$ is in °K and $(p_0)_{perf}$ is in atmospheres. The values of h_0 and s_0/R are calculated using the real nitrogen formulas of Ref. 12.

Charts of the equivalent perfect gas supply temperature and pressure, $(T_0)_{perf}$ and $(p_0)_{perf}$, are shown in Figs. 8 and 9, respectively. These charts and other data for computing the equilibrium flow of real nitrogen will be contained in a forthcoming VKI report.[14]

Figures 8 and 9 show that the equivalent perfect gas supply conditions are generally much higher than the actual values. This is due to the storage of energy in intermolecular forces, and in vibrational excitation, which is released as the flow expands. The importance of these effects may be illustrated by the following example. In a facility operating at a supply temperature of 2000°K and a supply pressure of 200,000 psi, Figs. 8 and 9 show that $(T_0)_{perf}/T_0 = 1.75$ and $p_0/(p_0)_{perf} = 4$. The test section temperature is therefore 1.75 times higher than that which would result from operation at the same value of T_0 at low supply pressures, and the onset of condensation is delayed to higher Mach numbers. Furthermore, at the test section Mach number at which the static temperature has fallen to the condensation threshold, the static pressure (and Reynolds number) will correspond to a perfect gas expansion from 4 × 200,000 = 800,000 psi. Dense gas effects therefore greatly increase the Reynolds number attainable with a reservoir of a given structural strength.

Aside from illustrating the benefits incurred by dense gas effects, the charts of Figs. 8 and 9 have great practical utility in data reduction, since once the equivalent perfect gas supply conditions are found, existing supersonic flow tables may be employed to compute all the test section flow parameters of interest.

The dense-gas isentropic nozzle expansion theory has been confirmed over a limited range of operating conditions by test section Pitot and static pressure calibrations. The static pressures were measured on a flat plate at a nominal Mach number of 15 in conical flow and corrected for hypersonic interaction effects.[15] The static pressures agreed with predictions based on the measured supply and Pitot pressures with an average error of ±4%. The data was obtained during a test in which the supply pressure and temperature varied from 11,800 to 31,200 psi and 1692 to 2150°K, respectively. A full check of the theory will be possible with the new reservoir, which is designed for operation at pressures up to 200,000 psi.

V. Conclusions

Real gas effects caused by a high flow density play an important role in facilities that operate at very high pressures. Good agreement has been obtained between theoretical calculations and experimental measurements of the piston cycle and reservoir pressure decay in Longshot, which employs nitrogen test and driver gases. The theory also shows that the flow conditions in the test section correspond to equivalent perfect gas values of supply temperature and pressure which may be much higher than the actual values. This is due to the release, during the expansion process, of energy stored in intermolecular forces and vibrational excitation.

References

[1] Richards, B. E. and Enkenhus, K. R., "The Longshot Free-Piston Hypersonic Tunnel," VKI TN 49, Sept. 1968, von Kármán Institute for Fluid Dynamics, Rhode-Saint-Genèse, Belgium.

[2] Perry, R., "The Longshot Type of High-Reynolds Number Tunnel," 3rd Hypervelocity Techniques Symposium, Denver, Colo., March 1964.

[3] Boison, C. J., "Longshot I—Hypersonic Free Piston Tunnel," RAC 1884A, Dec. 1963, Republic Aviation Corp., Farmingdale, L.I.

[4] Humphrey, B. G., Jr., Panunzio, S., and Pinkus, O., "A Theoretical and Experimental Investigation of the Free-Piston Cycle," AFFDL-TR-66-204, Jan. 1967, Air Force Flight Dynamics Lab., Dayton, Ohio.

[5] Enkenhus, K. R. and Parazzoli, C., "The Longshot Free-Piston Cycle. Part I—Theory," VKI TN 51, Nov. 1968, von Kármán Institute for Fluid Dynamics, Rhode-Saint-Genèse, Belgium.

[6] Gaydon, A. G. and Hurle, I. R., *The Shock Tube in High-Temperature Chemical Physics*, Reinhold, New York, 1963.

[7] Stalker, R. J., "An Approximate Theory of Gun Tunnel Behaviour," *Journal of Fluid Mechanics*, Vol. 22, Pt. 4, 1965, pp. 657–670.

[8] Siegel, A. E., "The Theory of High-Speed Guns," AGARDograph 91, May 1965, NATO.

[9] Parazzoli, C. and Enkenhus, K. R., "The Longshot Free-Piston Cycle. Part II—Comparison of Theory with Experiment," VKI TN 52, Dec. 1968, von Kármán Institute for Fluid Dynamics, Rhode-Saint-Genèse, Belgium.

[10] Enkenhus, K. R., "On the Pressure Decay Rate in the Longshot Reservoir," VKI TN 40, 1967, von Kármán Institute for Fluid Dynamics, Rhode-Saint-Genèse, Belgium.

[11] Phinney, R., "Criterion for Vibrational Freezing in a Nozzle Expansion," *AIAA Journal*, Vol. 1, No. 2, Feb. 1963, pp. 496–497.

[12] Culotta, S. and Enkenhus, K. R., "Analytical Expressions for the Thermodynamic Properties of Dense Nitrogen," VKI TN 50, Dec. 1968, von Kármán Institute for Fluid Dynamics, Rhode-Saint-Genèse, Belgium.

[13] Grabau, M. and Brahinsky, H. S., "Thermodynamic Properties of Nitrogen from 300°K to 5000°K and from 1 to 1000 Amagats," AEDC-TR-66-69, Aug. 1966, Arnold Engineering Development Center.

[14] Culotta, S. and Richards, B. E., "Charts and Formulas for Determining Flow Conditions in Real Nitrogen Expanding Flows," VKI TN 58, Jan. 1970, von Kármán Institute for Fluid Dynamics, Rhode-Saint-Genèse, Belgium.

[15] Bailey, F. R., "Flat Plate Pressure Distribution and Heat Transfer in a Conical Hypersonic Flow," VKI TN 56, Jan. 1970, von Kármán Institute for Fluid Dynamics, Rhode-Saint-Genèse, Belgium.

JANUARY 1970 AIAA JOURNAL VOL. 8, NO. 1

Investigation of Supersonic Phenomena in a Two-Phase (Liquid-Gas) Tunnel

ROBERT B. EDDINGTON*
Air Force Institute of Technology, Wright-Patterson Air Force Base, Ohio

Homogeneous two-phase flows of dispersed liquid and gas having gas-to-liquid volume ratios around 1:1 exhibit the characteristics of a continuum flow with a greatly reduced sound propagational velocity. This velocity approaches 66 fps at atmospheric pressure for a homogeneous mixture of water and air, and reduces further as the square root of the static pressure. Flows of such mixtures at velocities in excess of the local velocity of sound can produce shock phenomena similar to that experienced in supersonic, gaseous media. A supersonic two-phase tunnel was designed and built to create normal and oblique shock structure that can be photographed and analyzed with a minimum of boundary-layer interference. The applicability of the isothermal continuum theory to such flows is confirmed empirically for volume ratios near 1:1. Auxiliary flow devices were constructed for the measurement of such difficult to determine flow parameters as the relative phase velocity, local void ratio, coefficient of friction, and stagnation pressure. A general change in the flow model matrix was found at volume ratios approaching 1:1. The coefficient of friction measured for supersonic flow was found to be a simple function of the local void ratio. Stagnation pressures measured for a wide range of flow conditions approximate an isentropic relation for a substantial part of the supersonic flow spectrum. Measurements of flow characteristics were made over a range of Mach numbers from 2.2 to 19.

Nomenclature

c = velocity of sound (fps)
M = Mach number
m = mass (slug/ft^3)
P = mixture pressure (lbf/ft^2)
P_3 = isentropic stagnation pressure, mixture (lbf/ft^2)
P_4 = normal shock plus isentropic stagnation pressure, mixture (lbf/ft^2)
r_m = gas-to-liquid mass ratio
r_v = gas-to-liquid volume ratio
u = X component of mixture velocity (fps)
$\bar{u}$ = component of mixture velocity normal to the shock wave (fps)
u' = component of mixture velocity parallel to inclined plane (fps)
v = downstream velocity component perpendicular to the upstream flow direction (fps)
$\mathcal{V}$ = volume (ft^3)
V = velocity (fps)
β = angle of shock wave with horizontal (deg)
θ = angle of inclined plane with the horizontal (deg)
ρ = mixture density (slug/ft^3)

Received January 31, 1969; revision received July 11, 1969. Portions of the results were presented as Paper 66-87 at the 3rd Aerospace Sciences Meeting, New York, January 24–26, 1966. The work was supported by the Jet Propulsion Laboratory of the California Institute of Technology. Technical monitors of the effort were D. G. Elliott of the Research and Advanced Concepts Section, Jet Propulsion Laboratory, and H. J. Stewart of the Department of Aeronautics, California Institute of Technology.

* Associate Professor of Mechanical Engineering; currently Staff Development Engineer, Directorate of Operational Requirements and Development Plans, DCS/R&D, HQ USAF, Washington, D. C.; Lt. Colonel U.S. Air Force.